Geothermics 125 (2025) 103146

Contents lists available at ScienceDirect

Geothermics

journal homepage: www.elsevier.com/locate/geothermics

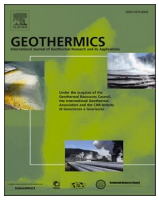

GeoProp: A thermophysical property modelling framework for single and two-phase geothermal geofluids

Tristan Merbecks [a,b,*], Allan M.M. Leal [b], Paola Bombarda [a], Paolo Silva [a], Dario Alfani [a], Martin O. Saar [b]

[a] Department of Energy, Politecnico di Milano, Italy
[b] Geothermal Energy and Geofluids Group, Institute of Geophysics, Department of Earth and Planetary Sciences, ETH Zurich, Switzerland

ARTICLE INFO

Keywords:
Geofluids
Thermophysical properties
Phase behaviour
Geothermal energy

ABSTRACT

The techno-economic evaluation of geothermal resources requires knowledge of the geofluid's thermophysical properties. While the properties of pure water and some specific brines have been studied extensively, no universally applicable model currently exists. This can result in a considerable degree of uncertainty as to how different geothermal resources will perform in practice. Geofluid modelling has historically been focused on two research fields: 1) partitioning the geofluid into separate phases, and 2) the estimation of the phases' thermophysical properties. Models for the two fields have commonly been developed separately. Recognising their potential synergy, we introduce *GeoProp*, a novel geofluid modelling framework, which addresses this application gap by coupling existing state-of-the-art fluid partitioning simulators, such as *Reaktoro*, with high-accuracy thermophysical fluid property computation engines, like *CoolProp* and *ThermoFun*. *GeoProp* has been validated against field experimental data as well as existing models for some incompressible binary fluids. We corroborate GeoProp's efficacy at modelling the thermophysical properties of geothermal geofluids via a case study on the heat content of different geofluids. Our results highlight the importance of accurately characterising the thermophysical properties of geofluids in order to quantify the resource potential and optimise the design of geothermal power plants.

1. Introduction

Over the coming decades the global energy industry will be exposed to considerable external pressures. On the one hand energy demand is rising as a result of population growth and the continuing improvements in the global standard of living and quality of life. Simultaneously, supply is transitioning away from fossil fuels to carbon-free energy sources, due to concerns over global climate change (IEA, 2021). Considering this, technologies tapping into Earth's natural, vast and renewable energy reserves, such as wind, solar and geothermal energy, have emerged as cost-effective and clean alternatives for all final energy uses (IEA, 2021).

Specifically, geothermal energy is proving to be an attractive and versatile option for grid-scale renewable and dispatchable electricity and heat generation. To date, geothermal energy utilisation has mostly been limited to high-temperature hydrothermal systems, typically located at tectonic plate boundaries (e.g. Iceland, Indonesia and New Zealand). However, the adoption of binary ORC (Organic Rankine Cycle) technologies has widened the applicability range of geothermal power generation to other geographic locations (e.g. Germany) that exhibit lower enthalpy, liquid-dominated resources (DiPippo, 2016).

In a binary geothermal power plant, the hot geofluid (single- or two-phase) is used to heat and evaporate a secondary low-boiling-point fluid. The resultant vapour is then expanded via a turbine, driving a generator to generate electricity, before being condensed, repressurised and recirculated, thus forming a closed loop (Fig. 1).

This closed-cycle configuration has several operational advantages over traditional open-cycle Flash geothermal power plants. Primarily, ORC turbines tend to be smaller, cheaper and more efficient as well as have longer life spans when compared to analogous steam turbines (DiPippo, 2016). Furthermore, the distinct closed-cycle configuration of binary power plants provides another operational advantage by ensuring that critical plant equipment (e.g. turbine) remains unexposed to the frequently corrosive and geochemically unstable geofluids (i.e. scaling).

For instance, by being able to select the working fluid for a binary cycle, it is possible to avoid wet expansion in the turbine, which is

* Corresponding author.
E-mail address: tristanleonard.merbecks@polimi.it (T. Merbecks).

https://doi.org/10.1016/j.geothermics.2024.103146
Received 28 February 2024; Received in revised form 27 July 2024; Accepted 16 August 2024
Available online 4 October 2024

Nomenclature

Symbol

a	Activity, -
b	Elemental amount, Mol
G	Gibbs free energy, J
h	Partial molar enthalpy, J/mol
$\overline{h}$	Specific enthalpy, J/kg
H	Enthalpy, J
m	Mass, kg
Mr	Molecular mass, kg/mol
n	Amount, mol
N	Number of species, -
P	Pressure, Pa
Q	Heat, J
R	Universal gas constant, J/mol/K
s	Partial molar entropy, J/mol/K
$\overline{s}$	Specific entropy, J/kg/K
S	Entropy, J/K
T	Temperature, K
U	Internal energy, J
v	Partial molar volume, m^3/mol
V	Volume, m^3
w	Stoichiometric coefficient, mol/mol
W	Work, J
x	Mass fraction, -
y	Mole Fraction, -
α	Vapour Fraction, mol/mol
μ	Chemical Potential, J/mol
ρ	Density, kg/m^3
ψ	Placeholder property, Property/kg

Superscript

$^\circ$	Standard state
G	Gaseous Phase
L	Liquid/Aqueous Phase
sat	Saturated fluid
S	Solid/Mineral Phase
T	Total Phase

Subscript

$geofluid$	Geofluid
i	Species i
j	Species j
$salt$	Salts
$water$	Pure Water

Accent

BIC	binary interaction coefficient
EOS	equation of state
NCG	non-condensable gases
ORC	organic Rankine cycle
PHE	primary heat exchanger
PR	Peng-Robinson
SRK	Soave-Redlich-Kwong
VLE	vapour-liquid equilibrium
WP	Wagner-Pruß

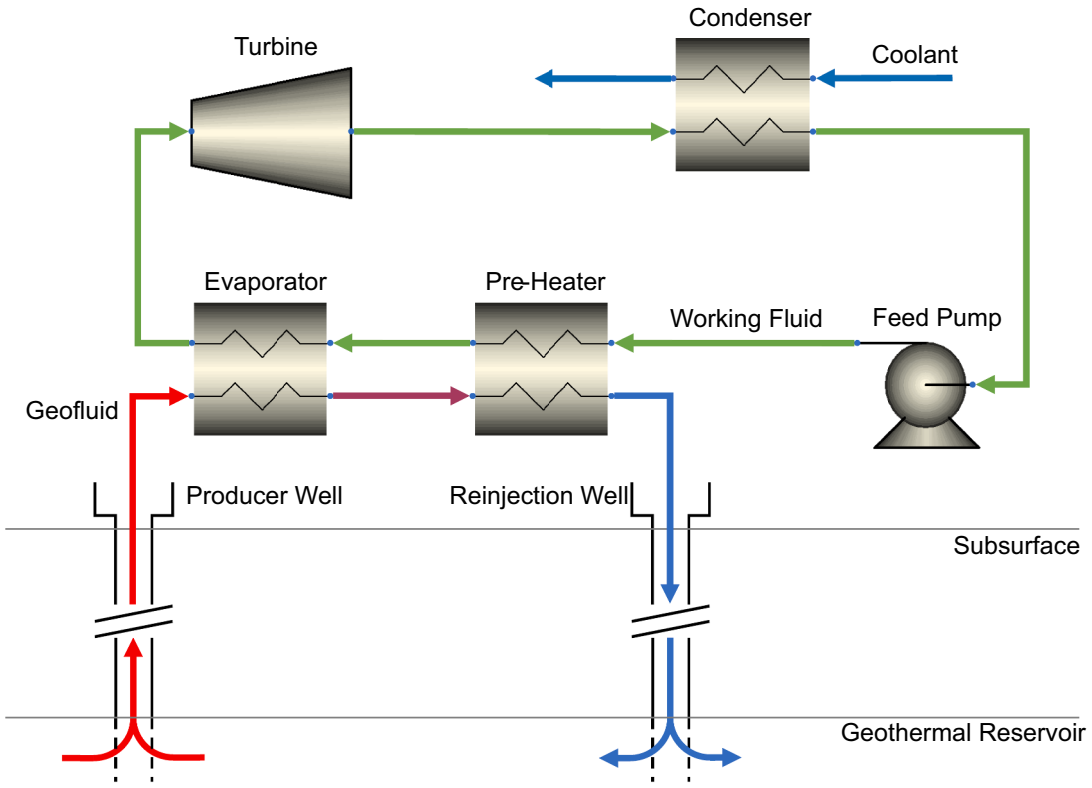

Fig. 1. Process schematic of a geothermal binary ORC power plant. The hot geofluid heats and evaporates a secondary fluid (cycle working fluid). While the cold geofluid is reinjected into the reservoir, the now gaseous cycle working fluid is expanded in a turbine, which in turn drives a generator to produce electricity. The low-pressure vapour is condensed and then repressurised before being re-fed to the pre-heater, closing the cycle.

unavoidable in direct steam cycle geothermal power plants, due to the bell-shaped water vapour dome in the temperature-entropy domain. Wet expansion results not only in reduced efficiency but the formation of droplets, due to condensation, also damages the turbine interior.

Closed-cycle configurations, however, come at the expense of reducing the potential for useful work being extracted from the geofluid, also referred to as the geofluid's exergy. These exergetic losses are particularly prevalent during the primary heat introduction (i.e. across the pre-heater and evaporator), leading to a reduction in the overall conversion efficiency.

Algorithms and expertise already exist in the industry to minimise such exergetic losses, resulting from the extensive experience of operating ORCs in related applications, such as heat recovery as well as waste-to-energy and biomass-to-energy conversion – the main difference being the heat source. However, key inputs, such as the geofluid phase behaviour and thermophysical properties, are expensive to obtain experimentally, while no holistic and predictive models currently exist. Thus, we must often rely on mathematical models and equations of state as well as on calibrating model parameters according to experimental and field observations.

2. Scope

The simulation of geothermal energy systems (i.e. reservoir, wells, production network and power plant) requires accurate knowledge of the thermophysical properties of the geofluid. For example, calculations involving fluid dynamics, heat transfer and/or expansion/compression processes require both thermodynamic properties (e.g. density, specific enthalpy, specific entropy, etc.) and transport properties (e.g. viscosity and thermal conductivity).

The geofluid composition, minimum and maximum temperature as well as the maximum pressure in the geothermal system are all location-specific. On the other hand, the minimum pressure is primarily dependent on the power plant configuration (e.g. direct steam cycles expand the geofluid to low pressures in the turbine, whereas in binary cycles the geofluid only experiences comparatively small pressure losses in the heat exchangers).

For a model to be applicable to a wide range of geothermal resources and power plant configurations, the allowable temperatures and pressures should, at a minimum, range from 15 °C to 250 °C and 0.08 bar (i.e. the condenser pressure in direct steam cycles) to 300 bar, respectively (DiPippo, 2016). Moreover, the geofluid composition should be adaptable to include the most common mineral and non-condensable gases (NCG) found in geothermal systems.

3. Modelling approaches

Depending on the geofluid composition and the modelling objectives, different modelling approaches for predicting the thermophysical properties can be applied.

3.1. Pure fluids

Fluids primarily comprised of a single component can, under some circumstances, be approximated as a pure fluid of the primary constituent. Thus, geothermal geofluids, which are primarily composed of water, could be approximated as pure water. The phase behaviour and thermophysical properties of pure water have been studied extensively and high-fidelity equations of state (EOS) have been developed to calculate its thermophysical properties for a wide range of conditions temperatures and pressures. The current industry standard formulation is that developed by Wagner-Pruß (WP) (IAPWS, 2018; Wagner and Pruß, 2002).

Similar EOS have also been developed for other common constituents of geofluids, such as carbon dioxide (Span and Wagner, 1996), nitrogen (Span et al., 2000), methane (Setzmann and Wagner, 1991) and hydrogen sulphide (Lemmon and Span, 2006).

These pure component EOS can also be used to model mixtures of said pure components, provided that models that capture the interactions between the constituent components have also been developed. One such approach is the use of binary interaction coefficients (BICs), which are obtained by calibration against experimental data (Bell and Lemmon, 2016). However, this approach cannot be used to capture chemical reaction between pure components.

CoolProp (Bell et al., 2014) is an open-source framework for calculating thermophysical properties of fluids and implements the aforementioned pure component EOS and BICs. *REFPROP* (Lemmon et al., 2018) and *FluidProp* (Colonna et al., 2019) are two other popular calculation frameworks that implement many of the same models, however, both are commercial tools, and as such represent black boxes.

Table 1
The applicability range of various EOS for binary incompressible fluids.

Fluid	T_{min}, °C	T_{max}, °C	x_{min}	x_{max}
Seawater	0	120	0	0.12
Lithium Bromide	−0.15	226.85	0	0.75
Calcium Chloride	−55	20	0.15	0.3
Potassium Carbonate	−100	40	0	0.4

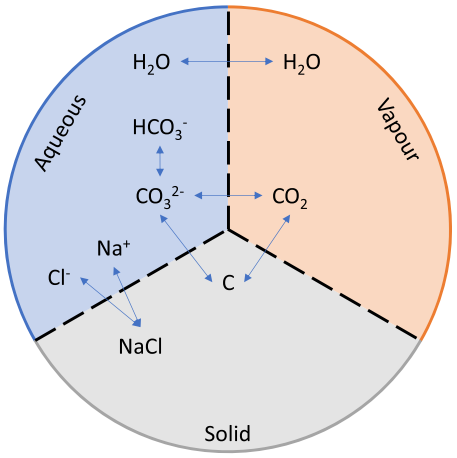

Fig. 2. Schematic of a possible chemical reactive system describing a geofluid.

3.2. Incompressible binary fluids

Furthermore, EOS have also been developed for some industrially relevant mixtures, like seawater (Sharqawy et al., 2010), lithium bromide solution (Pátek and Klomfar, 2006), and calcium chloride solution (Preisegger et al., 2010) or potassium carbonate solution (Melinder, 2010). However, the application range of such binary incompressible fluid EOS is limited, Table 1, due to the scope in which these fluids are used /handled in industry (e.g. seawater in desalination plants or lithium bromide in adsorption cooling). Moreover, no interaction models exist to allow mixtures of these binary mixtures (e.g. seawater and lithium bromide) or binary mixtures with other pure components (e.g. seawater and carbon dioxide) to be modelled. EOS for the aforementioned incompressible binary fluids are also available in *CoolProp*.

3.3. Chemically reactive systems

An alternative approach is to treat the geofluid as a chemically reactive system. In such a system, the constituent species can partition into different phases (e.g. gaseous, aqueous – a water-rich liquid phase, or solid), react with each other to form new species or dissociate into other species (Fig. 2). Determining the amounts and composition of all

phases at equilibrium, at a given temperature and pressure, is equivalent to assessing the geofluid's phase behaviour and also allows the thermophysical properties of the individual phases and overall fluid to be obtained.

A unit amount of geofluid of arbitrary overall composition can be approximated as a closed thermodynamic system (i.e. no mass transfer into or out of the system). From the Second Law of Thermodynamics, such systems reach equilibrium when the system entropy reaches a global maximum. For systems at constant temperature and pressure, it can be shown that this is consistent with the Gibbs free energy, Eq. (1), of the system reaching a global minimum, Appendix A: Chemical Equilibrium.

$$G = H - TS \tag{1}$$

Thus, determining the equilibrium state (i.e. finding the phase amounts and compositions) represents a minimisation problem (i.e. $\underset{\boldsymbol{n}}{min} G(P,\ T,\ \boldsymbol{n})$), subject to the constraint that the total mass of each chemical element (i.e. H, O, Na, Cl, etc.) is conserved across all species and phases considered (i.e. $\sum_i^N w_{ij} n_i = b_j$, where w_{ij} is the number of atoms of element j that make up species i, n_i is the amount of species i, and b_j is the total amount of element j in the system).

A convenient expression for calculating the Gibbs free energy of the system can be obtained by combining the differential form of the Gibbs free energy (at constant temperature and pressure), Eq. (2), with the First Law of Thermodynamics (i.e. $dU = \delta W + \delta Q + \Sigma \mu_i dn_i$), assuming fully reversible processes (i.e. $\delta Q = TdS$) and mechanical work (i.e. $\delta W = pdV$), followed by integration over the molar amounts. This allows the Gibbs free energy of the system to be calculated from the amounts of each species and their respective chemical potential (Eq. (3)). Here, G is Gibbs free energy, P is pressure, T is temperature, U is internal energy, V is volume, S is entropy, μ_i is the chemical potential of species i, n_i is the number of moles of species i and $\boldsymbol{y}$ is the vector of all species' mole fractions.

$$dG|_{P,\ T} = dU + PdV - TdS \tag{2}$$

$$G(P,T) = \sum_i^N n_i \mu_i(P,\ T,\ \boldsymbol{y}) \tag{3}$$

The partial derivatives of the chemical potential are the partial molar enthalpy, Eq. (4), the partial molar entropy, Eq. (5), and the partial molar volume, Eq. (6), - the thermodynamic properties of interest.

$$h_i(T,\ P,\ \boldsymbol{y}) = \left.\frac{\partial(\mu_i(T,\ P,\ \boldsymbol{y})/T)}{\partial(1/T)}\right|_{P,\ \boldsymbol{y}} \tag{4}$$

$$s_i(T,\ P,\ \boldsymbol{y}) = -\left.\frac{\partial \mu_i(T,\ P,\ \boldsymbol{y})}{\partial T}\right|_{P,\ \boldsymbol{y}} \tag{5}$$

$$v_i(T,\ P,\ \boldsymbol{y}) = \left.\frac{\partial \mu_i(T,\ P,\ \boldsymbol{y})}{\partial P}\right|_{T,\ \boldsymbol{y}} = \frac{1}{\rho_i(T,\ P,\ \boldsymbol{y})} \tag{6}$$

The calculation of the chemical potential is broken down into two components; the standard chemical potential of the species at a reference state, and the species' activity, Eq. (7). The species' activity is defined as the difference between the actual chemical potential and the standard chemical potential (Eq. (8)).

The reference state is chosen by convention: For liquid or gaseous species, the reference composition, $\boldsymbol{y}^\circ$, is that of the pure component, whereas for aqueous species (e.g. Na^+), a 1-molal solution of the solute is chosen, with all other species at infinite dilution. Meanwhile, the reference pressure for liquid and aqueous species is taken as the system pressure (i.e. $P^\circ = P$), whereas for gases, the reference pressure is taken to be 1 bar (i.e. $P^\circ = 1$ bar).

$$\mu_i(P,T,\boldsymbol{y}) = \mu_i(P^\circ,T,\boldsymbol{y}^\circ) + RT\ln a_i(P,T,\boldsymbol{y}) \tag{7}$$

$$RT\ln a_i(P,T,\boldsymbol{y}) \equiv \mu_i(P,T,\boldsymbol{y}) - \mu_i(P^\circ,T,\boldsymbol{y}^\circ) \tag{8}$$

With the above in mind, determining the equilibrium composition and thermophysical properties of a geofluid at a given temperature and pressure requires three inputs: 1) The amounts of all elements across all species, 2) the chemical potential of all species at their respective reference state (also called the standard chemical potential) and 3) the activity of all species.

The elemental amounts can be obtained from the geofluid composition, which is specific to each geothermal site as it is dependent on several factors, such as reservoir rock composition, temperature and pressure. Thus, the geofluid composition can only reliably be obtained from geofluid samples.

The species' standard chemical potential can be obtained from peer-reviewed open-source databases, such as SUPCRT92 (Johnson et al., 1992) or SUPCRTBL (Zimmer et al., 2016). Frameworks, such as *ThermoFun* (Miron et al., 2021) and *Reaktoro* (Leal, 2015), implement several models for computing standard thermodynamic properties from such databases. Alternatively, high-fidelity EOS for species, such as water and carbon dioxide, can be used. Computationally cheaper EOS, such as Soave-Redlich-Kwong (SRK) or Peng-Robinson (PR), can be used, provided their input parameters (e.g. critical properties, acentric factor, etc.) have been calibrated to the specific component in question.

The species' activity can be calculated from phase and species-specific activity models. The simplest activity models approximate the fluid as an ideal fluid (i.e. Ideal Gas, Ideal Solution or Ideal Solid). However, this approach limits their application to low concentrations (for Ideal Solutions) or low pressures and high temperatures (for Ideal Gases), where the species exhibit ideal behaviour and where interactions amongst molecules are negligible. For gaseous species, such as CH_4, N_2, H_2S, etc., SRK or PR EOS may also be used to approximate the real gas behaviour and interactions amongst other gaseous species.

Various activity models have been proposed for the different types of aqueous species. For example, the Setschenow equation (Setschenow, 1889) for neutral species, the HKF-Debye-Hückel model (Helgeson et al., 1981) for water and ionic species, or the Pitzer model for various aqueous species (Pitzer and Mayorga, 1973). Moreover, species-specific activity models have been developed for common mixtures of species. For example, for mixtures of H_2O, CO_2, CH_4 and some mineral species, models by Duan and Sun as well as Spycher and Pruess, amongst others, can be used (Duan and Sun, 2003; Spycher et al., 2003; Spycher and Pruess, 2009). The selection of an activity model is ultimately dependent on the species present, their relative amounts as well as the system temperature and pressure.

Reaktoro (Leal, 2015) is a unified open-source framework for modelling chemically reactive systems. *Reaktoro* pairs the aforementioned thermodynamic databases, EOS and activity models with scalable optimisation algorithms (Leal et al., 2017) and on-demand machine learning acceleration strategies (Kyas et al., 2022; Leal et al., 2020). Reaktoro was used in Walsh et al. (2017) to produce a computer code to compute both thermodynamic and thermophysical properties, such as viscosity and thermal conductivity. The core *Reaktoro* calculation engine is written in C++ for performance reasons, with Python API provided for more convenient usage in Jupyter Notebooks and/or with the rich ecosystem of Python libraries.

In principle, chemically reactive systems allow any number of species and reactions to be modelled. However, the main barrier to this approach, being applied universally to geofluid modelling in a geothermal context, is the availability of appropriate activity models for all species - particularly gaseous water (i.e. steam). While the WP EOS represents the highest fidelity model for the properties of water and steam (IAPWS, 2018), it is computationally expensive and it only works with a single component: water. For this reason, most geochemical modelling codes (e.g., PHREEQC, GEMS, Reaktoro) adopt cubic equations of state for the vapour phase, such as the Peng-Robinson EOS or the Soave-Redlich-Kwong EOS, to permit other gases such as CO_2, H_2S, O_2,

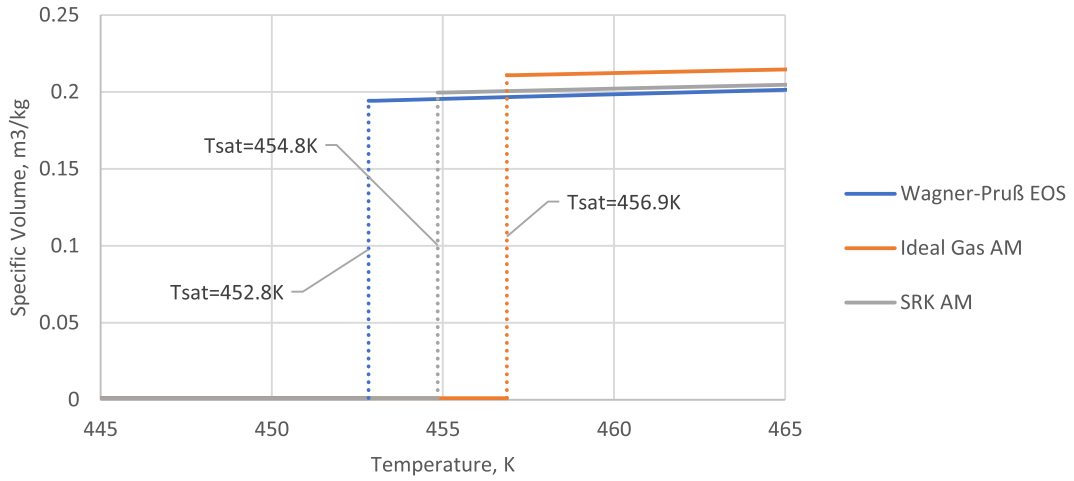

Fig. 3. The specific volume of pure water at a pressure of 10 bar over temperatures 445–465 K calculated with Reaktoro (Leal, 2015) using the Ideal Gas and Soave-Redlich-Kwong (SRK) EOS, compared to the Wagner-Pruß EOS (Wagner and Pruß, 2002).

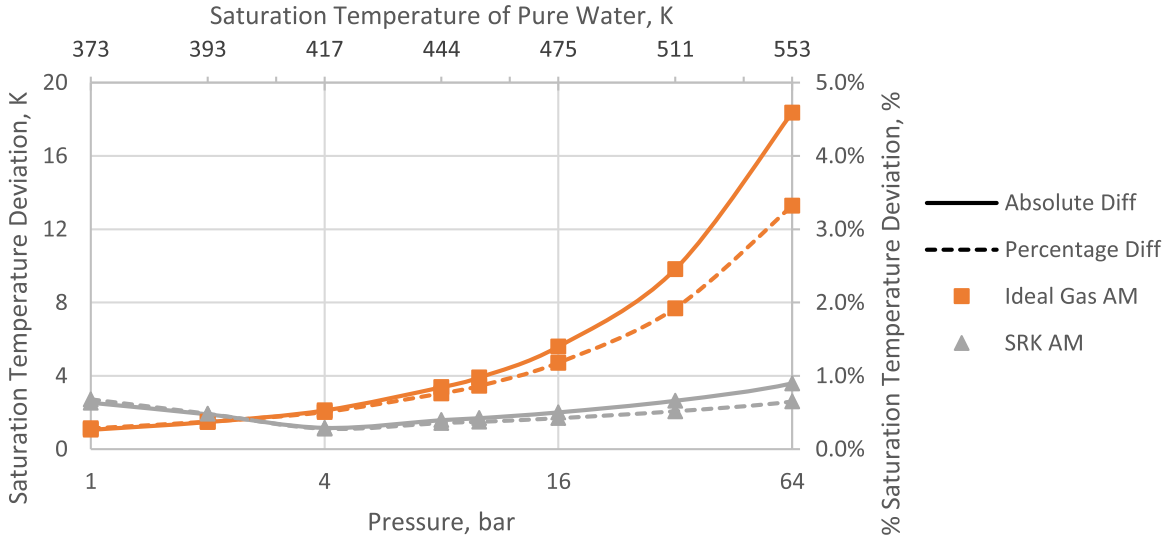

Fig. 4. The deviation of saturation temperature (from the Wagner-Pruß EOS) when computed as part of a VLE calculation in Reaktoro (Leal, 2015) assuming either the ideal gas and SRK EOS for the vapour phase and the SUPCRTLBL thermodynamic database (Zimmer et al., 2016).

and others to be considered. However, this can result in deviations from the expected phase behaviour when water steam is in higher proportion compared to other gases or simply the only gaseous species.

For example, for pure water at a pressure of 10 bar the WP EOS predicts a saturation temperature of around 453 K. To model the same fluid using a chemically reactive system we assume a system consisting of only an aqueous and a gaseous water species (i.e. H_2O(aq) and H_2O (g). This system was then simulated in Reaktoro, as part of a vapour-liquid-equilibrium (VLE) calculation, for a pressure of 10 bar and a temperature between 445 K and 465 K. The SUPCRTBL database was used for the standard thermodynamic properties and different EOS (ideal gas and SRK) as activity models for the vapour phase (i.e., H_2O (g)). The specific volume of the fluid was evaluated for each state and compared against values calculated via the WP EOS (Fig. 3). In the case of Reaktoro, the saturation temperature was inferred by the temperature at which the transition from liquid-like to vapour-like densities occurs. The Python script is available on GitHub (https://github.com/EASYGO-ITN/GeoProp/tree/main/PaperResources).

Depending on the equation of state selected in Reaktoro, the specific volume differs from the values predicted by the WP EOS by 1.3% (SRK) and 6.5% (Ideal Gas) (Fig. 3). These differences indicate that the partial derivatives of the chemical potential (in this case with respect to pressure) of gaseous water equation [6], are inconsistent with the WP EOS. Consequently, in direct steam cycle geothermal power plants, the steam turbine would be designed and optimised for different volumetric rates and velocities, resulting in sub-optimal turbine designs.

Furthermore, the transition from liquid-like to vapour-like specific volume occurs at higher temperatures compared to WP EOS, indicating that the selected EOS (i.e., SRK and Ideal Gas) result in the chemical potential of gaseous water to be overestimated. By definition, at saturation, the chemical potential of the same chemical species in different phases is the same (i.e. $\mu_i^L = \mu_i^G$).

Although the differences in saturation temperature are small in relative terms (less than 0.7% in the case of the SRK activity model), the absolute differences (2 K in the case of the SRK activity model), when compared to key power plant design parameters, such as the minimum approach temperature difference in the heat exchange equipment (typically between 5 K and 10 K), are significant, representing differences of 20% to 40%. This can affect the required heat transfer area, which is the primary driver for the cost of heat exchange equipment.

Repeating the above experiment for different system pressures (Fig. 4), for the SRK activity model, the deviations range between 0.28%

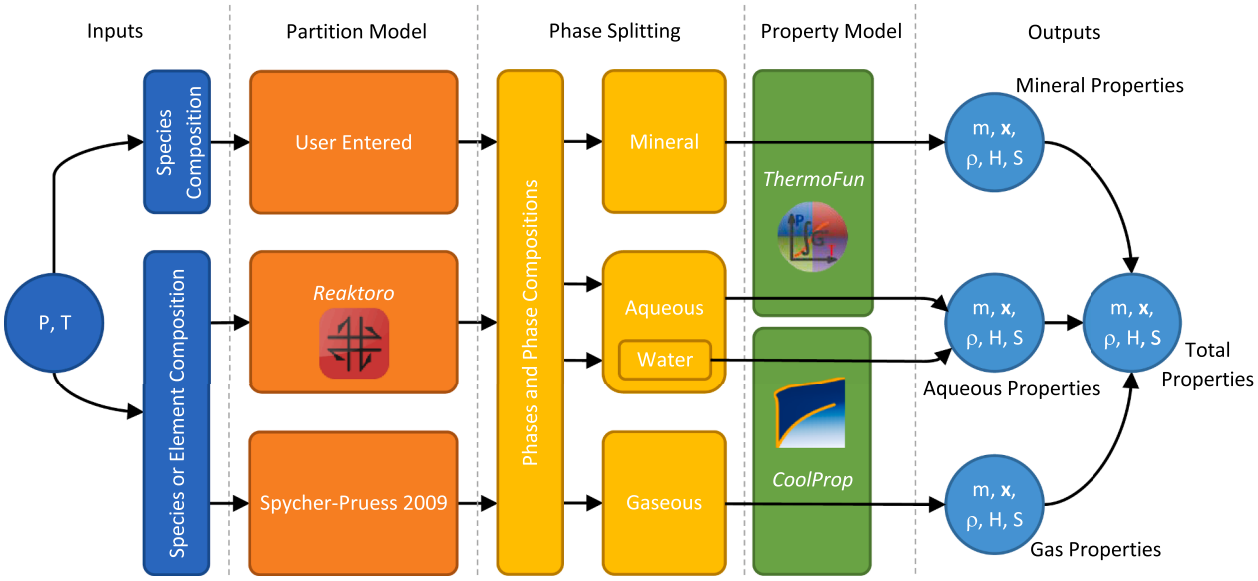

Fig. 5. The calculation architecture of GeoProp for partitioning geofluids and calculating their thermophysical properties.

and 0.68% in relative terms, and 1.16 K to 3.6 K in absolute terms, while for the Ideal Gas activity model the saturation temperature deviation increases from 0.28% (corresponding to 1.06 K) at 1 bar to 3.32% (corresponding to 18.4 K) at 64 bar. The latter can be explained by the deviation from ideal gas behaviour at elevated pressures. Thus, for pressures exceeding 2.5 bar (corresponding to a saturation temperature of 400 K for pure water), the SRK activity model provides more accurate saturation temperature estimates than the Ideal Gas activity model. The Python script is available on GitHub (https://github.com/EASYGO-ITN/GeoProp/tree/main/PaperResources).

3.4. Empirical models for geofluids

Empirical models for specific geofluid mixtures, most commonly for mixtures comprised of water, and carbon dioxide as well as impurities, such as CH_4, N_2 and H_2S, have been developed. An example of this is a model originally presented by Spycher and Pruess (2003) for the mutual solubilities of carbon dioxide and water at low temperatures (12 °C-100 °C). This model was later extended to higher temperatures (12 °C to 300 °C) by Spycher and Pruess (2009). Corrections for salinity are applied using an approach similar to that of Duan and Sun (2003).

While such empirical models can be used to determine equilibrium phases and compositions, they do not provide methods for estimating the thermophysical properties of the fluid. Moreover, these models make simplifying assumptions, particularly regarding the reactivity of the various aqueous species, meaning that advanced phase behaviours, such as scaling/mineralisation, cannot be captured.

4. GeoProp

The aforementioned frameworks/models fall into two categories: partition models for determining the number, amounts and composition of equilibrium phases; and property models for estimating the thermophysical properties of fluids of known composition. GeoProp was developed in recognition of these synergies and allows different partitioning and property frameworks/models to be coupled with another (Fig. 5), all while maintaining the flexibility of customising the underlying calculation engines.

The main underlying data structure, "Fluid", is a container for the compositional data of the geofluid. The individual species are stored in "Phases", both in their native phase (i.e. aqueous, gaseous or mineral) and in a total phase, capturing all species. The "Fluid" can be passed from one calculation engine (e.g. partition model or property model) to another, with the required input data and parameters being automatically passed to the underlying models. The user defines the initial species and their total amounts. The phase compositions are populated after performing a partitioning calculation, while the thermophysical properties are updated following the property calculation.

The "Partition" module equilibrates an input "Fluid" and partitions the "Fluid" into the equilibrium phases. This determines the number, amounts and composition of the equilibrium phases at the given temperature and pressure. Two partition models are available: a) *Reaktoro* and b) Spycher-Pruess (2009) (Appendix B: Spycher-Pruss, 2009 Phase Partitioning Model provides details of its implementation). However, the open architecture of GeoProp allows other partition models to be included. Additionally, the user retains the ability to fully customise the underlying equilibrium and partitioning calculations, such as selecting non-default activity models in *Reaktoro*.

The "Property" module evaluates the properties of a given "Fluid" at the specified pressure and temperature. This module currently uses two calculation engines: a) *CoolProp* and b) *ThermoFun*.

The properties of gaseous phase species are evaluated in *CoolProp* using a mixture of pure components and the default BIC data. In case of non-convergence, an ideal mixture is assumed (i.e. mixture effects are negligible), allowing the pure component properties to be calculated and then aggregated to the phase properties.

ThermoFun is used to calculate the properties of all aqueous species besides water, which is calculated using *CoolProp's* implementation of the WP EOS. Aqueous species are assumed to be dilute and hence mixture effects are insignificant (i.e. unit activity for all aqueous species), which allows the pure component properties, ψ_i^L, to be used. In turn, the ψ_i^Ls are then aggregated to the overall aqueous phase properties, Eq. (9) and Eq. (10). ψ_i^L is a placeholder for properties such as the species' enthalpy, entropy or density.

$$\psi_i^L(T,P,\boldsymbol{y}) = \frac{1}{Mr_i} * \left[\partial\mu_i(P,T,\boldsymbol{y}^\circ) + RT\,\partial\underbrace{\left(\ln a_i(P,T,\boldsymbol{y})\right)}_{=0\ as\ a_i\cong 1}\right] \tag{9}$$

$$\psi^L(T,\ P,\ \boldsymbol{y}) = \frac{\sum_i^N m_i^L * \psi_i^L}{\sum_i^N m_i^L} \tag{10}$$

Mineral phase properties are computed with *ThermoFun*, assuming that each mineral constitutes a separate pure phase. Thus, unit activities are assumed, allowing the pure component properties, ψ_i^S, to be used, which are then aggregated to the overall mineral phase properties,

Table 2
The composition of the geothermal fluid samples near Makhachkala (Abdulagatov et al., 2016). Species exclusively below the detection threshold of 0.1 mg/L have been omitted.

Species		Sample No. 68 mg/L	Sample No. 129 mg/L	Sample No. 27T mg/L
Cations	B	1.2	2.4	59.3
	Ba	<0.1	<0.1	1.7
	Ca	49.2	2.8	73.6
	K	10.2	4.7	145
	Li	0.2	0.1	2.2
	Mg	32.9	1.3	28.5
	Na	396	590	7540
	P	<0.1	0.2	<0.1
	S	240	211	39.8
	Se	2.4	0.2	<0.1
	Si	13.8	12.3	29.4
	Sr	1.1	0.1	6.7
Anions	Cl	152	276	7387
	SO4	749	616	30.7
Total		**1662.7**	**1830.0**	**15,345.9**

Eq. (11) and Eq. (12).

$$\psi_i^S(T,P,\boldsymbol{y}) = \frac{1}{Mr_i} * \left[\partial\mu_i(P,T,\boldsymbol{y}^\circ) + RT\,\partial\left(\ln a_i(P,T,\boldsymbol{y})\right)^{=0\ as\ a_i\cong 1}\right] \tag{11}$$

$$\psi^S(T,\ P,\ \boldsymbol{y}) = \frac{\sum_i^N m_i^S * \psi_i^S}{\sum_i^N m_i^S} \tag{12}$$

The properties of all phases are aggregated to the overall fluid properties employing a mass-fraction-based mixing rule, Eq. (13).

$$\psi^T(T,\ P,\ \boldsymbol{y}) = \frac{\sum_j^N m^j * \psi^j}{\sum_j^N m^j} \tag{13}$$

GeoProp is fully open-source, and is accessible on GitHub (https://github.com/EASYGO-ITN/GeoProp) and Zenodo (https://zenodo.org/records/10676479).

5. Validation

We use geofluid samples, collected from geothermal fields near Makhachkala, Dagestan in Russia, by Abdulagatov et al. (2016) as the primary validation dataset. This dataset includes the fluid density, speed of sound and specific enthalpy (inferred from density and speed of sound measurements) for various temperatures. The composition of the fluid samples is summarised in Table 2. The salinity of these fluids ranges between about 1.5 $g_{Minerals}$/L to 16 $g_{Minerals}$/L.

We also consider several "synthetic" datasets. For example, seawater is a good analogue for simple geothermal brines as it is primarily comprised of water and NaCl. Although lithium bromide is not typically present in large quantities in geothermal fluids, it is also considered to test the applicability of GeoProp to unconventional brines. The thermophysical properties of these fluids were obtained from the MITSW and LiBr incompressible binary mixture EOS, implemented in *CoolProp*. Moreover, with these EOS, it is possible to explore a wider range of salinities and temperatures.

A final benchmark is performed against the ELECNRTL electrolyte model in *ASPEN Plus V11*, a common process simulation software.

The fluids were recreated in GeoProp and *Aspen Plus*, and then equilibrated over a range of temperatures, determining their thermophysical properties (Figs. 6 and 7), the Python script is available un GitHub (https://github.com/EASYGO-ITN/GeoProp/tree/main/Paper

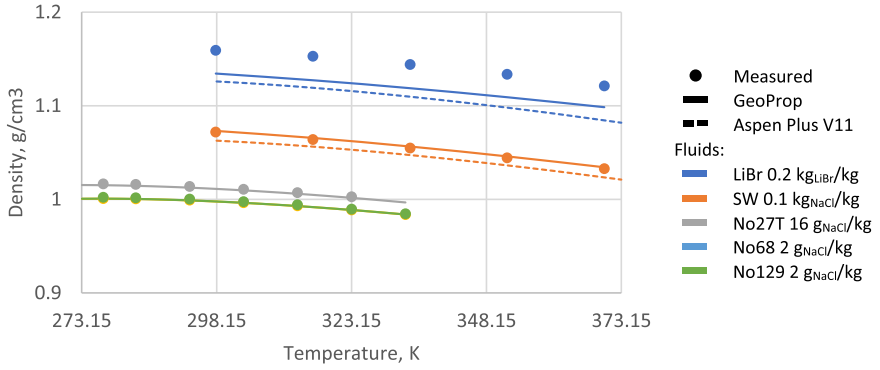

Fig. 6. The density of various brines as a function of temperature at 1 bar pressure. Solid circles represent "measured" data and lines represent property models.

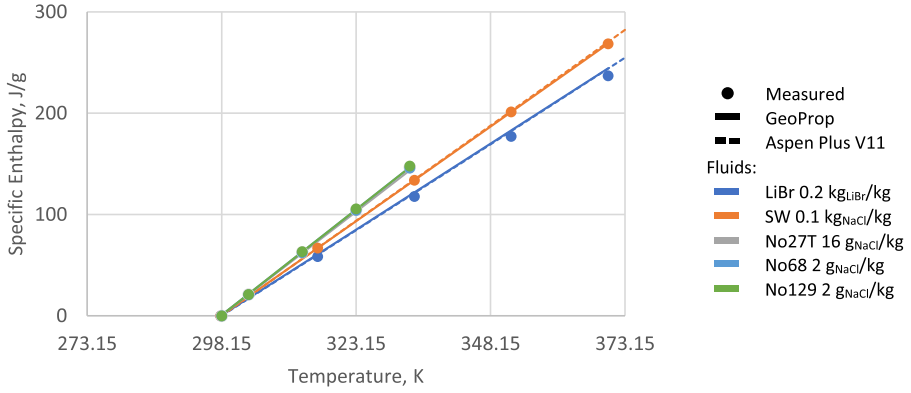

Fig. 7. The specific enthalpy of various brines as a function of temperature at 1 bar pressure. The reference temperature is 25 °C. Solid circles represent "measured" data and lines represent property models.

Table 3
Used compositions and models of the considered geofluids.

		Units	Geofluid			
			Water	Brine	Water & NCG	Brine & NCG
Component:	H_2O	mass	100	95	95	90
	NaCl	%	–	5	–	5
	CO_2		–	–	5	5
Partition Model		–	WP EOS (*CoolProp*)	*Reaktoro*	Spycher-Pruess	Spycher-Pruess
Property Model		–	Default – i.e. *ThermoFun* & *CoolProp*			

Resources). We find that GeoProp reproduces the "measured" densities of all fluids at all temperatures to within 3%, narrowly outperforming the ELECNRTL model in *Aspen Plus*. For the specific enthalpy, both GeoProp and *Aspen Plus* reproduced the measurements to within 1%.

6. Case study

A common approach for investigating the comparative performance of different geothermal power plant technologies is to treat the geofluid as pure water. However, this approach neglects the impact impurities, such as dissolved salts and non-condensable gases (NCG), can have on the phase behaviour and thermophysical properties.

These differences can be illustrated by considering the primary heat exchanger (PHE) in a simple binary ORC geothermal power plant (Fig. 1) and calculating the heat released by different geofluids as a function of reinjection temperature. Four geofluids (Table 3) are considered and their temperature heat-content (TQ) curves are generated in GeoProp (Fig. 8), the Python script is available un GitHub (https://github.com/EASYGO-ITN/GeoProp/tree/main/PaperResources).

The inlet conditions are defined in terms of a common temperature of 473 K and a heat content of 1135 kJ/kg, relative to 298 K and 101,325 Pa. The heat content corresponds to that of pure water at 473 K and a vapour quality of 20 mass%. The same inlet temperature has been considered in order to investigate similar geothermal heat sources, while the heat content has been fixed to have Primary Heat Exchangers units of similar capacity. The vapour quality and inlet pressure are calculated in GeoProp. The resulting inlet conditions are summarised in Table 4.

Unlike "Water", "Brine" experiences a small temperature glide in the two-phase region as condensing water reduces the effective salinity of the aqueous phase, thereby reducing the saturation temperature. Moreover, liquid "Brine" has a lower specific heat capacity than liquid "Water", as indicated by the steeper slope.

Thus, a binary ORC operating on a liquid-dominated "Brine"-like geofluid has a higher cycle working fluid mass rate to geofluid mass rate ratio compared to a "Water"-like geofluid. Consequently, for the same net power, a higher mass rate of the "Brine"-like geofluid is required. In turn, the higher geofluid mass rate also affects the heat exchanger design, in particular the required heat transfer and cross-sectional areas and, hence, the cost.

Above 440 K, the specific heat capacity of "Water & NCG" deviates from "Water" significantly, which can be attributed to the presence of NCG, reducing the boiling point of the geofluid, allowing the water species to remain in the vapour phase at lower temperatures. For example, at the inlet, the vapour quality of "Water & NCG" is 26.5 mass %, compared to just 20 mass% for "Water". Discounting the initial NCG content of 5 mass%, this means that an additional 1.5 mass% of water is in the vapour phase. Similarly, when the vapour quality of "Water" reaches zero, "Water & NCG" still has a vapour quality of 9 mass%, implying that about 4 mass% of water still remains in the vapour phase.

The curvature of the TQ curve for "Water & NCG" (Fig. 8) also has practical implications, as it reduces the average temperature difference between the hot geofluid and the cold working fluid, compared to the "Water" case. This increases the heat transfer area required and, in turn, the cost of the heat exchanger.

The "Brine & NCG" case has a slightly higher vapour quality, compared to the "Water & NCG" case. This can be attributed to the presence of Na^+ and Cl^- ions.

7. Conclusions

There are several modelling approaches that can be used for predicting the phase-behaviour and thermophysical properties of geothermal geofluids. However, these approaches tend to focus on either modelling the phase partitioning or the fluid phase properties. We present a novel framework for modelling the thermophysical properties of

Table 4
Inlet conditions of the geofluids considered.

Conditions	Units	Geofluid			
		Water	Brine	Water & NCG	Brine & NCG
Inlet: Mass Rate	kg/s			1	
Temperature	K			473	
Heat Content	kJ/kg			1135	
Pressure	bar	15.55	14.4	16.53	16.26
Vapour Quality	mass%	20.0	22.3	26.5	31.8

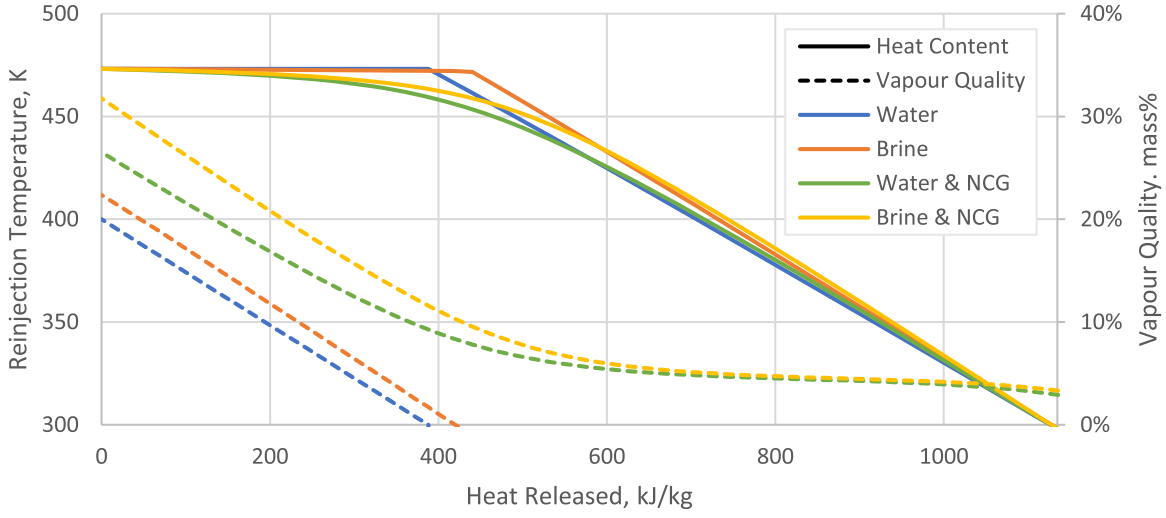

Fig. 8. The temperature and heat released by different geofluids as well as the corresponding vapour quality. The heat content is relative to 298 K and 101,325 Pa.

geothermal brines, GeoProp, which couples existing partitioning and property models, extending their individual capabilities. The approach presented, allows the thermophysical properties and phase behaviour of geothermal brines for a wide range of temperatures, pressures and compositions to be calculated, which are required for the accurate simulation, and the proper design and evaluation, of direct steam cycle or binary cycle geothermal power plants. GeoProp is available on GitHub (https://github.com/EASYGO-ITN/GeoProp) under an Apache License 2.0 license.

CRediT authorship contribution statement

Tristan Merbecks: Conceptualization, Methodology, Software, Validation, Data curation, Writing – original draft, Visualization. **Allan M.M. Leal:** Writing – original draft. **Paola Bombarda:** Writing – original draft, Funding acquisition. **Paolo Silva:** Writing – original draft. **Dario Alfani:** Writing – original draft, Conceptualization. **Martin O. Saar:** Writing – original draft, Supervision, Funding acquisition.

Declaration of competing interest

The authors declare that they have no known competing financial interests or personal relationships that could have appeared to influence the work reported in this paper.

Data availability

The authors have included the links to the corresponding Github and Zenodo repositories are provided in the Manuscript.

Acknowledgements

The EASYGO project (easygo-itn.eu) has received funding from the European Union's Horizon 2020 Research and Innovation Programme under the Marie Skłodowska-Curie grant agreement no 956965.

A. M. M Leal and M. O. Saar thank the Werner Siemens Foundation (Werner Siemens-Stiftung) for its support of the Geothermal Energy and Geofluids (geg.ethz.ch) Group at ETH Zurich, Switzerland, as well as the Energi Simulation Foundation (energisimulation.com) for partial funding of this research.

The contributions by D. Alfani were carried out within the NEST - Network 4 Energy Sustainable Transition (D.D. 1243 02/08/2022, PE00000021) and received funding under the National Recovery and Resilience Plan (NRRP), Mission 4 Component 2 Investment 1.3, funded from the European Union - NextGenerationEU. This manuscript reflects only the authors' views and opinions, neither the European Union nor the European Commission can be considered responsible for them.

Appendix A. Chemical equilibrium

For a closed system under isothermobaric conditions, equilibrium is established when the Gibbs free energy reaches a global minimum (Gyftopoulos and Beretta, 2005). The Gibbs free energy, G, is defined in Eq. (14), where H is enthalpy, S is entropy and T is absolute temperature.

$$G = H - TS \tag{14}$$

Eq. (15) gives the differential form of Eq. (14), where U is internal energy, P is absolute pressure and V is volume. At constant temperature and pressure, Eq. (15) reduces to Eq. (16).

$$dG = dU + PdV + VdP - TdS - SdT \tag{15}$$

$$dG|_{P,\,T} = dU + PdV - TdS \tag{16}$$

The change in internal energy can be attributed to either a heat or work interaction, see Eq. (17), where δQ is heat added to the system and δW is the work done on the system. The work done captures both mechanical (i.e. pressure-volume) and non-mechanical (e.g. electromagnetic) work, see Eq. (18), where δW_x is non-mechanical work.

$$dU = \delta Q + \delta W \tag{17}$$

$$\delta W = -PdV + \delta W_x \tag{18}$$

Substituting Eq. (17) and Eq. (18) into Eq. (16), reduces the differential form of the Gibbs free energy to Eq. (19).

$$dG|_{P,\,T} = \delta Q + \delta W_x - TdS \tag{19}$$

Since $Q \leq TdS$, from the second law of thermodynamics, it follows that $Q - TdS \leq 0$, yielding Eq. (20), meaning that in the absence of non-mechanical work (i.e. $\delta W_x = 0$) the change in Gibbs free energy is strictly negative, see Eq. (21). Hence, as the system approaches equilibrium, the Gibbs free energy tends towards a global minimum.

$$dG|_{P,\,T} \leq \delta W_x \tag{20}$$

$$dG|_{P,\,T} \leq 0 \tag{21}$$

From the second law of thermodynamics, equilibrium is established when the entropy of the system no longer changes (i.e. $dS = 0$). The Gibbs free energy also provides a derived equilibrium condition, whereby equilibrium (at constant temperature and pressure for closed systems) is established when the Gibbs Energy no longer changes (i.e. $dG = 0$).

Appendix B. Spycher-Pruss 2009 phase partitioning model

We implemented the model for computing the mutual solubilities of water and carbon dioxide based on Spycher and Pruess, 2009 . Only the calculation of the fugacity coefficient has been altered, as there appears to be a typographic error in the original paper, which confuses k_{ij} with K_{ij} in their Equation A-8, Eq. (22). The fugacity coefficient should thus be calculated as follows, with K_{ij} evaluated from their Equation A-7.

$$\ln\Phi_k = \frac{b_k}{b_{mix}}\left(\frac{PV}{RT}-1\right)-\ln\left(P\frac{V-b_{mix}}{RT}\right)+\left(\frac{a_{mix}}{b_{mix}RT^{1.5}}\right)\ln\left(\frac{V}{V+b_{mix}}\right) \left(\frac{\sum_{i=1}^{n}y_i(a_{ik}-a_{ki})-\sum_{i=1}^{n}\sum_{j=1}^{n}y_i^2y_j\left(K_{ij}-K_{ji}\right)\sqrt{a_ia_j}+y_k\sum_i^n y_i(K_{ki}-K_{ik})\sqrt{a_ia_k}}{a_{mix}}-\frac{b_k}{b_{mix}}\right) \quad (22)$$

The revised Spycher-Pruss 2009 model can then be used to calculate the mole fraction of water in the carbon-dioxide-rich phase and the mole fraction of carbon dioxide in the water-rich phase. Subsequently, a mole balance is used to estimate the vapour fraction, α, Eq. (23). Note, z_{H_2O} is the mole fraction of water across all phases.

$$\alpha = \frac{z_{H_2O}-x_{H_2O}}{y_{H_2O}-x_{H_2O}} \quad (23)$$

If $\alpha < 0$, the geofluid is entirely liquid, i.e. all carbon dioxide is contained within the water-rich phase. If $0 < \alpha < 1$, the geofluid is a two-phase mixture and the water and carbon dioxide rich phases coexist in equilibrium. If $\alpha > 1$ or the pressure is below the saturation pressure of pure water at the given temperature, the geofluid is entirely vapour, i.e. all water is contained within the carbon dioxide rich phase.

References

Abdulagatov, I.M., Akhmedova-Azizova, L.A., Aliev, R.M., Badavov, G.B., 2016. Measurements of the density, speed of sound, viscosity and derived thermodynamic properties of geothermal fluids from south Russia Geothermal Field. Part II. Appl. Geochem. 69, 28–41. https://doi.org/10.1016/j.apgeochem.2016.04.003.

Bell, I.H., Lemmon, E.W., 2016. Automatic fitting of binary interaction parameters for multi-fluid Helmholtz-energy-explicit mixture models. J. Chem. Eng. Data 61 (11), 3752–3760. https://doi.org/10.1021/acs.jced.6b00257.

Bell, I.H., Wronski, J., Quoilin, S., Lemort, V., 2014. Pure and pseudo-pure fluid thermophysical property evaluation and the open-source thermophysical property library coolprop. Ind. Eng. Chem. Res. 53 (6), 2498–2508. https://doi.org/10.1021/ie4033999.

Colonna, P., Van Der Stelt, T., Guardone, A., 2019. FluidProp (Version 3.1): A Program for the Estimation of Thermophysical Properties of Fluids.

DiPippo, R., 2016. Geothermal Power Plants, 4th ed. Butterworth-Heinemann. https://doi.org/10.1016/C2014-0-02885-7.

Duan, Z., Sun, R., 2003. An improved model calculating CO2 solubility in pure water and aqueous NaCl solutions from 273 to 533 K and from 0 to 2000 bar. Chem. Geol. 193 (3–4), 257–271. https://doi.org/10.1016/S0009-2541(02)00263-2.

Gyftopoulos, E.P., Beretta, G.P., 2005. Thermodynamics: Foundations and Applications. Dover Publications.

Helgeson, H.C., Kirkham, D.H., Flowers, G.C., 1981. Theoretical prediction of the thermodynamic behavior of aqueous electrolytes by high pressures and temperatures; IV, Calculation of activity coefficients, osmotic coefficients, and apparent molal and standard and relative partial molal properties to 600 °C and 5kb. Am. J. Sci. 281 (10), 1249–1516. https://doi.org/10.2475/ajs.281.10.1249.

IAPWS, 2018. Main IAPWS Thermodynamic Property Formulations. http://www.iapws.org/newform.html.

IEA, 2021. World Energy Outlook 2021. https://www.iea.org/reports/world-energy-outlook-2021.

Johnson, J.W., Oelkers, E.H., Helgeson, H.C., 1992. SUPCRT92: a software package for calculating the standard molal thermodynamic properties of minerals, gases, aqueous species, and reactions from 1 to 5000 bar and 0 to 1000 °C. Comput. Geosci. 18 (7), 899–947. https://doi.org/10.1016/0098-3004(92)90029-Q.

Kyas, S., Volpatto, D., Saar, M.O., Leal, A.M.M., 2022. Accelerated reactive transport simulations in heterogeneous porous media using Reaktoro and Firedrake. Comput. Geosci. 26 (2), 295–327. https://doi.org/10.1007/s10596-021-10126-2.

Leal, A.M.M., 2015. Reaktoro: An Open-Source Unified Framework For Modeling Chemically Reactive Systems. https://reaktoro.org.

Leal, A.M.M., Kulik, D.A., Smith, W.R., Saar, M.O., 2017. An overview of computational methods for chemical equilibrium and kinetic calculations for geochemical and reactive transport modeling. Pure Appl. Chem. 89 (5), 597–643. https://doi.org/10.1515/pac-2016-1107.

Leal, A.M.M., Kyas, S., Kulik, D., Saar, M.O., 2020. Accelerating reactive transport modeling: ondemand machine learning algorithm for chemical equilibrium calculations. Transp. Porous Med. 133, 161–204. https://doi.org/10.1007/s11242-020-01412-1.

Lemmon, E.W., Bell, I.H., Huber, M.L., McLinden, M.O., 2018. NIST Standard Reference Database 23: reference Fluid Thermodynamic and Transport Properties-REFPROP. Version 10.0, National Institute of Standards and Technology. https://doi.org/10.18434/T4/1502528.

Lemmon, E.W., Span, R., 2006. Short fundamental equations of state for 20 industrial fluids. J. Chem. Eng. Data 51 (3), 785–850. https://doi.org/10.1021/je050186n.

Melinder, Å., 2010. Properties of Secondary Working Fluids (Secondary Refrigerants or Coolants, Heat Transfer Fluids) for Indirect Systems, 2nd ed.

Miron, G.D., Kulik, D., Leal, A., Dmytrieva, S., 2021. ThermoFun: C++/Python code to fetch standard thermodynamic data from ThermoHub database. Goldschmidt2021 Abstr. https://doi.org/10.7185/gold2021.4489.

Pátek, J., Klomfar, J., 2006. A computationally effective formulation of the thermodynamic properties of LiBr–H2O solutions from 273 to 500K over full composition range. Int. J. Refriger. 29 (4), 566–578. https://doi.org/10.1016/j.ijrefrig.2005.10.007.

Pitzer, K.S., Mayorga, G., 1973. Thermodynamics of electrolytes. II. Activity and osmotic coefficients for strong electrolytes with one or both ions univalent. J. Phys. Chem. 77 (19), 2300–2308. https://doi.org/10.1021/j100638a009.

Preisegger, E., Flohr, F., Krakat, G., Glück, A., Hunold, D., 2010. D4 properties of industrial heat transfer media. VDI Heat Atlas. Springer Berlin Heidelberg, pp. 419–512. https://doi.org/10.1007/978-3-540-77877-6_20.

Setschenow, J., 1889. Über die Konstitution der Salzlösungen auf Grund ihres Verhaltens zu Kohlensäure. Zeitschrift Für Physikalische Chemie 4U (1), 117–125. https://doi.org/10.1515/zpch-1889-0409.

Setzmann, U., Wagner, W., 1991. A New equation of state and tables of thermodynamic properties for methane covering the range from the melting line to 625 K at pressures up to 100 MPa. J. Phys. Chem. Referen. Data 20 (6), 1061–1155. https://doi.org/10.1063/1.555898.

Sharqawy, M.H., Lienhard, J.H., Zubair, S.M., 2010. Thermophysical properties of seawater: a review of existing correlations and data. Desalinat. Water Treat. 16 (1–3), 354–380. https://doi.org/10.5004/dwt.2010.1079.

Span, R., Lemmon, E.W., Jacobsen, R.T., Wagner, W., Yokozeki, A., 2000. A reference equation of state for the thermodynamic properties of nitrogen for temperatures from 63.151 to 1000 K and pressures to 2200 MPa. J. Phys. Chem. Referen. Data 29 (6), 1361–1433. https://doi.org/10.1063/1.1349047.

Span, R., Wagner, W., 1996. A new equation of state for carbon dioxide covering the fluid region from the triple-point temperature to 1100 K at pressures up to 800 MPa. J. Phys. Chem. Referen. Data 25 (6), 1509–1596. https://doi.org/10.1063/1.555991.

Spycher, N., Pruess, K., 2009. A phase-partitioning model for CO_2–Brine mixtures at elevated temperatures and pressures: application to CO_2-enhanced geothermal systems. Transp. Porous Med. 82, 173–196. https://doi.org/10.1007/s11242-009-9425-y.

Spycher, N., Pruess, K., Ennis-King, J., 2003. CO2-H2O mixtures in the geological sequestration of CO2. I. Assessment and calculation of mutual solubilities from 12 to 100 °C and up to 600 bar. Geochim. Cosmochim. Acta 67 (16), 3015–3031. https://doi.org/10.1016/S0016-7037(03)00273-4.

Wagner, W., Pruß, A., 2002. The IAPWS Formulation 1995 for the thermodynamic properties of ordinary water substance for general and scientific use. J. Phys. Chem. Referen. Data 31 (2), 387–535. https://doi.org/10.1063/1.1461829.

Walsh, S.D.C., Garapati, N., Leal, A.M.M., Saar, M.O., 2017. Calculating thermophysical fluid properties during geothermal energy production with NESS and Reaktoro. Geothermics 70, 146–154. https://doi.org/10.1016/j.geothermics.2017.06.008.

Zimmer, K., Zhang, Y., Lu, P., Chen, Y., Zhang, G., Dalkilic, M., Zhu, C., 2016. SUPCRTBL: a revised and extended thermodynamic dataset and software package of SUPCRT92. Comput. Geosci. 90, 97–111. https://doi.org/10.1016/j.cageo.2016.02.013.